Study on Tsunami force for PC box girder

Yasuyuki Hirose[1]

Abstract

In this study, a waterway experiment was performed in order to understand the influence of tsunami forms on tsunami forces acting on the superstructure of standard the box girder. In the experiments, four types of tsunami waves were artificially generated: short period, long period, non-breaking abrupt and breaking abrupt wave, to act on a model bridge that simulated a real bridge superstructure in the waterway. Then, horizontal, vertical wave forces and moment were measured. As a result, the possibility that the different of forces due to tsunami shapes related to gradient of wave front was confirmed. In addition, the author converted experiment results to actual size tsunami forces and a simplified evaluation of washout safety of a real bridge by a tsunami was conducted.

Introduction

Many bridges were damaged by the tsunami associated with the Tohoku region Pacific Ocean earthquake that occurred on March 11, 2011 (hereinafter referred to as the Great East Japan Earthquake). Authorities such as national and prefectural governments have announced their predictions of earthquakes, including the soon-expected Nankai Trough Earthquake, and resulting floods due to large tsunami that will damage bridges. As shown in Pic. 1, there are bridges on the expressways in Japan that are close to the coast and may suffer tsunami damage.

In order to secure the transportation network in an emergency and implement appropriate maintenance of expressway, it is necessary to properly evaluate damage of bridges due to a tsunami.

However, at present, there are no rules and regulations for evaluating the impact of wave forces on bridges in the case of a tsunami as well as bridge safety against tsunami forces, including specifications for highway bridges. On the other hand, tsunami comes in various forms: for example, long-period waves with abrupt waves (bores) at the top end, and waves with breaking abrupt waves. Various forms of waves were witnessed in the Great East Japan Earthquake.[1), 2)] Therefore, it is easy to imagine that the types of tsunami vary depending on the location of a bridge upon which waves act.

In this study, a model bridge installed in the waterway was used and various artificially generated forms of waves assuming actual waves that would act on real bridges in order to understand the basic behavior of a tsunami load, and results of measurements of the waves, including short period solitary waves, long period solitary wave and abrupt waves (bores), are reported. In addition, wave forces that would act on

[1] Researcher, Bridge Division, Road Research Department, Nippon Expressway Research Institute Co., Ltd., Tokyo

real bridges were calculated based on the experiment results, and a simplified evaluation of washout safety of real bridges was made.

Pic.1 Bridge along the shore on an expressway

Waterway experiment

In the experiments, a visual waterway with a length of 20m, a cross-sectional width of 0.7m and a sectional height of 1.0m was used, as shown in Pic.2 and Fig.2. A tsunami was generated in the waterway; the tsunami waves were allowed to act on the experimental bridge model (hereafter, "model") simulating the bridge superstructure installed in the waterway and measurements of the forces acting on the model were carried out. As shown in Pic. 2, the model was a PC box-girder with one main girder to show water flows more simply than a steel plate-girder or a PCT-girder. The scales were either 1/50 or 1/100 as shown in Tab. 1 according to the types of tsunami. The model installed in the waterway was connected to the component force meter fixed by the supporting beam over the waterway; we used two under-the-girder heights: 100mm (1/50 scale) and 50mm (1/100 scale) to simulate 5m of the under-the-girder height from the static water level for a real bridge.

Tab. 2 shows types of tsunami waves used for the experiments. Four types of waves were used in total: short period waves, long period wave, non-breaking abrupt wave and breaking abrupt wave. In order to understand the basic behavior of the waves acting on the girder, solitary waves were used for all instances.

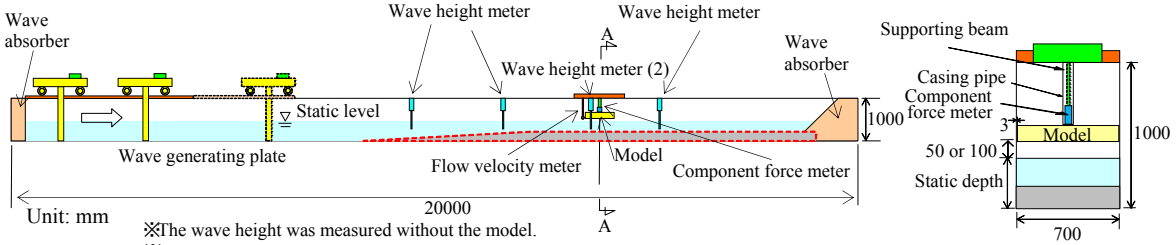

※The wave height was measured without the model.
※The wave height meter (2) was installed in the center of the model, although it is shown in a different position in the drawing.
※The distance from the static water level to the model was 50mm for the long period waves and breaking abrupt wave or 100m for the short period waves and non-breaking abrupt wave.
※The sampling frequency of the component force meter was 1000Hz.

Fig. 1 Lateral and Sectional Elevations of Experimental Waterway

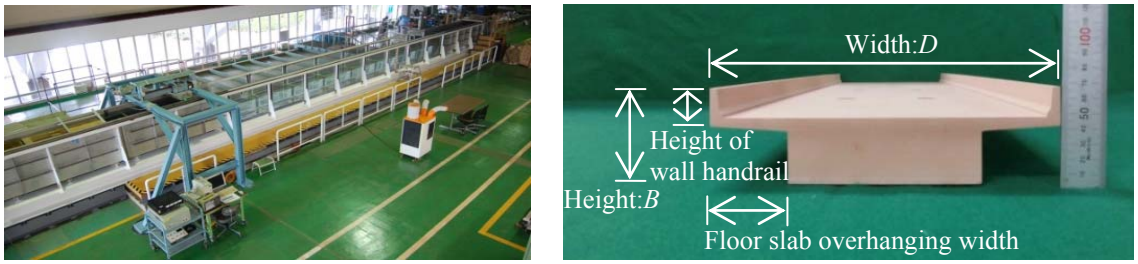

Pic.2 Waterway and section of model

Tab. 1 Proportion of model

	Actual scale bridge [m]	Model bridge [cm]	
Reduction scale	-	1/50	1/100
Width	11.64	23.3	11.6
Height	3.18	6.4	3.2
Height of wall handrail	1.28	2.6	1.3
Floor slab overhanging width	2.62	5.2	2.6
Weight [kN/m]	212	-	-

Tab. 2 Elements of Tsunami waves

Tsunami types	Model reduction scale	Height of tsunami h_a [cm]	Maximum flow velocity v_a [m/s]	Surface elevation velocity v_u [m/s]	Gradient of wave front θ [°]
Short period 1 wave	1/50	20	0.88	0.61	14.9
Short period 2 wave			0.96	0.64	16.4
Short period 3 wave			0.99	0.71	19.7
Long period wave	1/100	10	0.64	0.07	2.4
Non-Breaking abrupt wave	1/50	20	1.36	1.90	50.2
Breaking abrupt wave	1/100	10	2.22	0.05	1.0

Fig. 2 shows the definitions of wave elements. In this study, the wave abruptness was defined as Gradient of wave front θ, with the lower flange surface being an axis in order to comprehend the incident wave shape.

Then, assuming the maximum height of the tsunami wave is 10m for a actual scale bridge, the wave height of 20cm for the scale 1/50 and the wave height of 10cm for the scale 1/100 were used. Target waves were generated by controlling the travel and the speed of the wave generating plate of the sliding type and abrupt waves by installing

slope.

Measurement items were horizontal and vertical wave forces, and the flow force moment that acts on the model. The measurement was done by using the component force meter installed between the model and the supporting beam. In addition, the flow velocity and wave height were measured during a wave generation test as preparation before installing the model.

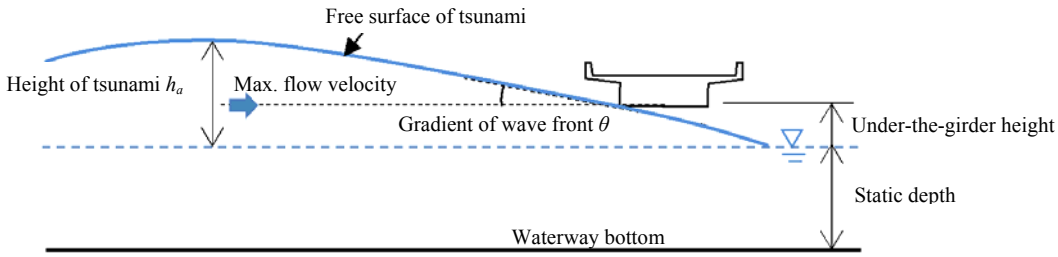

Fig. 2 Definition of elements

Measurement results of Tsunami force

Figures 3, 4 and 5 show the time histories of the first measurements for each wave type. For the horizontal wave force, the flow direction is positive; while for the vertical wave force the upward direction is positive. The horizontal axis indicates the start of the wave generating plate as 0 second. In addition, the side where the tsunami acts is defined as the front flow side, and the other side is defined as the rear flow side. Measurements were taken three times for each wave type, but because the characteristics of the maximum wave force and the time history were almost the same among three measurements, only the first measurement result is shown here.

Figures 3 and 4 show the first peak became the maximum value for both horizontal and vertical wave forces. However, for the horizontal wave force of breaking abrupt waves, the second peak had almost the same value as the first peak.

For the flow force moment, the first peak tended to be the maximum value, but for the long period wave, the second and the third peaks were close to the maximum value. In moment, the time history forms of the non-breaking and the breaking abrupt wave tended to be similar to those of the horizontal wave forces; this suggests possibility that the moment generated by the horizontal wave forces was dominant.

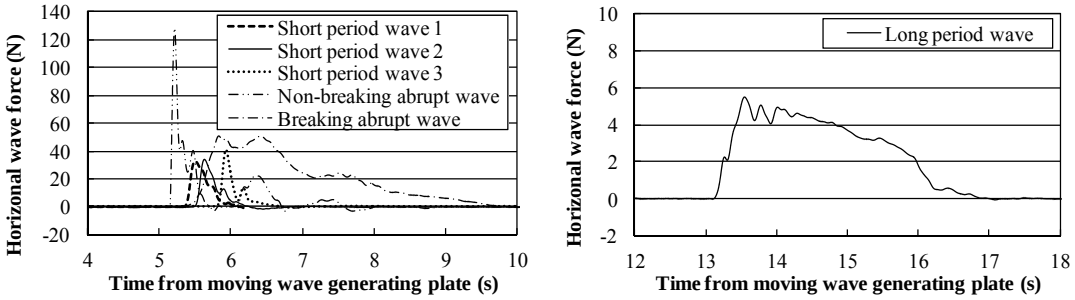

Fig. 3 Time history of horizontal wave force

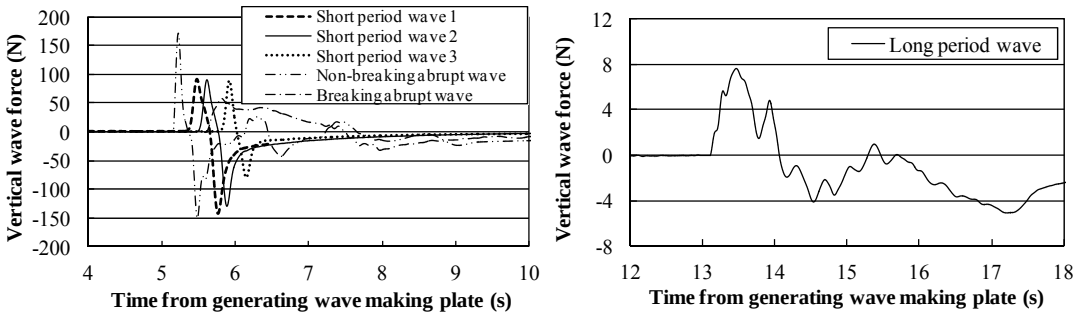

Fig. 4 Time history of vertical wave force

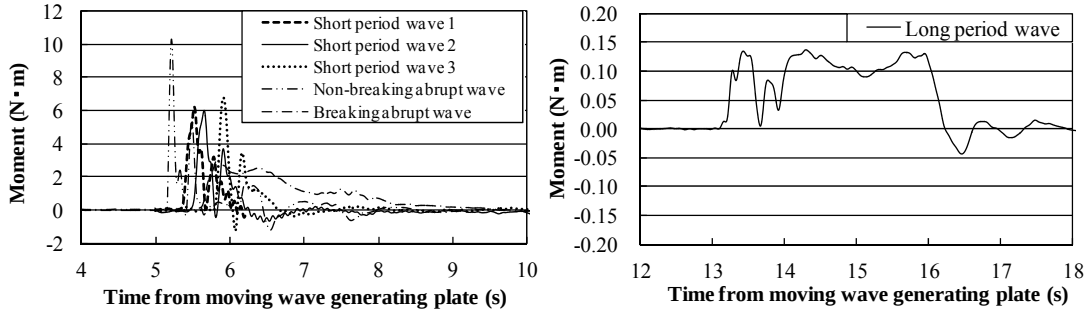

Fig. 5 Time history of moment

Pic.3 shows flow states around the sectional surface. The horizontal waves reached the peak while the space above the floor slab was submerged up to the wall handrail height after the slope of the water surface caused the waves to act on the front flow's side edge of either the bottom surface of the girder or the bottom surface of the girder and the overhanging floor slab. By this time, abrupt waves had already reached the other side of the wall handrail because of a faster flow velocity.

Then, the vertical upward waves increased their upward forces because of a rise in the water level and generated buoyancy and reached the maximum value before the tsunami covered the road surface. For the vertical downward wave forces, the short period waves and non-breaking abrupt wave reached the maximum value when the waves collided against the road surface on the superstructure and water flow was leaving from the girder and the floor slab on the bottom surface of the superstructure at the same time. On the other hand, the long period wave slowly passed over the wall handrail on the front flow side, while the breaking abrupt wave jumped over the wall handrail after act on it, and then a part of the wave started to cover the road surface. As described above, the waves were different in behavior when covering the road surface, but it's similar that both the long period wave and the breaking abrupt wave reached the maximum values with the passing of time, approximately when the road surface was submerged and the depth of water above the model became the deepest. Thus, we assumed that the different ways of the waves acting on the road surface and the phenomenon of the water flow leaving from the bottom of the girder and the floor slab had an effect on the short period waves and breaking abrupt wave reaching the clear peaks as well as the maximum values of the tsunami wave forces.

In addition, the flow force moment reached its maximum value when either the horizontal wave forces or the vertical upward wave forces became largest, as in Pic.3. However, the long period wave almost reached the maximum value even at the second or third peaks after the horizontal wave forces or the vertical upward wave forces became the largest.

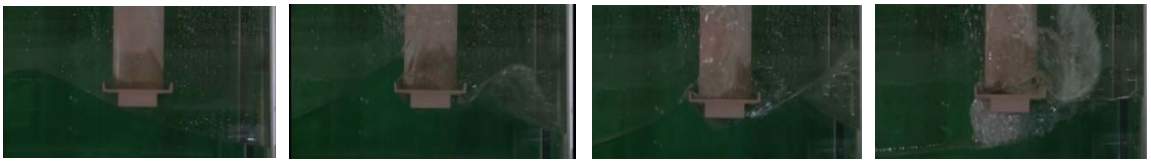

5.78s | 5.93s (Near the max. vertical upward wave force, horizontal wave force, and flow force moment) | 6.01s | 6.16s (Near the max. vertical downward wave force)

a) Short period wave (Case 3)

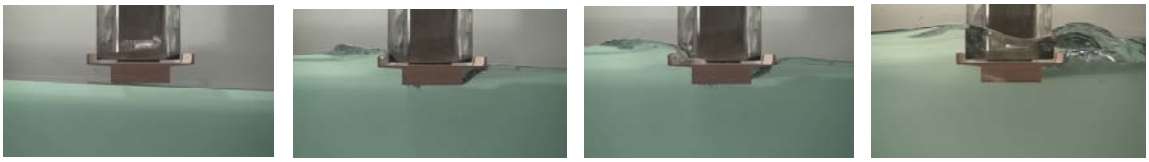

13.11s | 13.47s (The max. vertical upward wave force and flow force moment) | 13.55s (The max. horizontal wave force) | 14.53s (The max. vertical downward wave force)

b) Long period wave

5.15s | 5.20s (The max. horizontal wave force) and flow force moment | 5.21s (The max. vertical upward wave force) | 7.47s (The max. vertical downward wave force)

c) Non-breaking abrupt wave

5.40s | 5.82s (The max. vertical upward wave force, horizontal wave force, and flow force moment) | 6.40s (The second peak horizontal wave force) | 7.98s (The max. vertical downward wave force)

d) Breaking abrupt wave

Pic. 3 Flow state

Evaluation of hydrodynamic coefficient

Because the model scale and the tsunami flow velocity were not the same in the experiment, we used drag coefficient C_D, lift coefficient C_L and moment coefficient C_M to make the result dimensionless for evaluation. In general, a flow force coefficient is used to evaluate hydrodynamic force that acts on a structure in a steady flow, but we assumed the wave force at action on should be proportional to the square of the flow velocity.

$$C_D = \frac{2F_x}{\rho_w v_a{}^2 DL} \text{ ------ (1)} \qquad C_L = \frac{2F_z}{\rho_w v_a{}^2 BL} \text{ ------ (2)} \qquad C_M = \frac{2M_y}{\rho_w v_a{}^2 B^2 L} \text{ ------ (3)}$$

Where, ρ_w: Density of seawater
v_a: maximum flow velocity of wave without positioning the model at the specified position
D: Height of the model
B: Total width of the model
L: Length of the model

In addition, horizontal wave force F_x, vertical upward wave form F_z and flow force moment M were used the maximum values obtained by measurement.

Fig.6 shows the relationship between each component of the flow force coefficient (drag coefficient C_D, lift coefficient C_L and moment coefficient C_M) and the gradient of wave front resulting from calculations. Drag coefficient C_D tends to increase in proportion to the gradient of wave front. This way, it was observed that the drag coefficient has a correlation with the gradient of wave front regardless of wave types and horizontal wave forces can depend on the gradient of wave front, although the number of samples was still small. On the other hand, the lift coefficient and flow force moment tend to increase with an increase of the gradient of wave front in the range of smaller gradients, but they tend to remain on the same level after passing a certain range or to decrease.

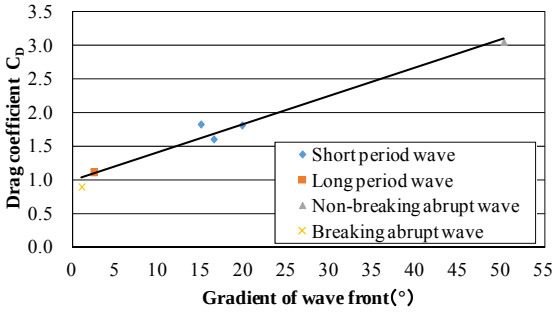

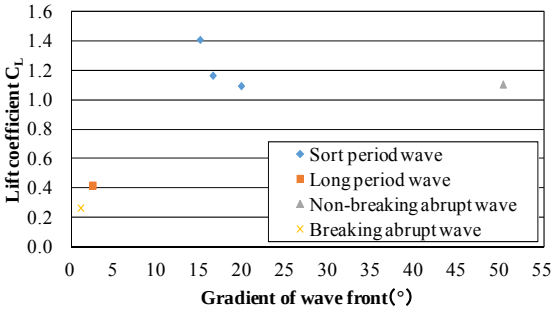

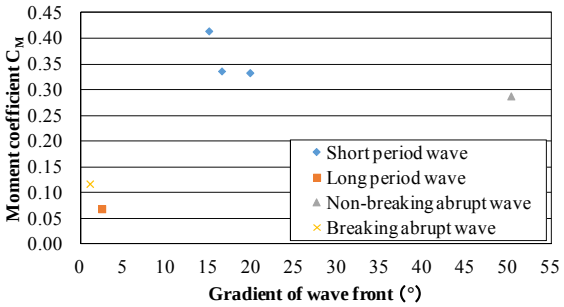

Fig.6 Relationship between hydrodynamic coefficient and gradient of wave front

Tsunami wave forces acting on a real bridge and evaluation of washout safety

We calculated tsunami wave forces acting on a actual scale bridge in order to define the differences of wave forces depending on tsunami types. The calculation process starts with solving the equations (1) to (3) above for wave forces and flow force moment, and then the wave forces were obtained by substituting the flow force coefficient previously calculated by the equations (1) to (3) as well as the actual scale bridge dimensions. In addition, it was assumed that the tsunami flow velocity v_a was set 6m/s as a reference based on the results of the images and numerical analysis in the Great East Japan Earthquake[1]. Tab. 3 shows the calculation results. As the table indicates, even if the flow velocity and the scale are the same, the wave forces are different greatly depending on the type of tsunami. In this experiment, the ratio of the maximum value to the minimum value became 3.4 times for the horizontal wave forces, 5.3 times for the vertical upward wave forces and 3.5 times for the flow force moment. In addition, the maximum vertical upward wave forces were larger than the maximum horizontal wave forces except for breaking abrupt wave.

Tab. 3 Maximum tsunami forces acting on an actual scale bridge
(The flow velocity unified as 6m/s.)

Wave force direction	Horizontal (kN/m)	Vertical upward (kN/m)	Flow force moment (kN・m/m)
Short period wave 1	107	236	1039
Short period wave 2	95	252	844
Short period wave 3	108	304	835
Long period wave	66	90	171
Non-breaking abrupt wave	180	239	722
Breaking abrupt wave	53	57	293

Tab. 4 shows the ratio of the tsunami wave forces acting on an actual scale bridge in Tab.3 to the dead load of the superstructure (212kN/m), β[3] obtained from the equation below, which was proposed by Kousa et al. to define washout risk of a bridge based on the ratio of resistance force *R* to acting force *D*.

$$\beta = \frac{R}{D} = \frac{\mu \cdot (W - F_{z\max})}{F_{x\max}} \quad \text{-------} \ (4)$$

Where, μ: Friction coefficient (=0.6[4] etc.)
W: Weight of girder
F_{xmax}: Maximum horizontal wave force
F_{zmax}: Maximum vertical upward wave force
If β>1, there will be no washout, and if β<1, there will be washout.

First, the ratio of the tsunami wave forces acting on an actual scale bridge to the weight of the superstructure is 0.1 to 0.9 for the horizontal direction. This ratio is smaller than the design seismic force (about 1.5) in specifications for highway bridges in Japan (for the third kind of ground – level 2 seismic vibration – type II). On the contrary, for the vertical direction, the ratio is larger than 0.3 in some cases; 0.3 is the lower limit of the design seismic force at the shoe in the vertical upward direction. Thus, it can be understood that the impact is more severe for the vertical than for the horizontal. From this finding, it is considered that the design seismic vibration level in the current quake-resistance standards is effective in the horizontal direction, but it is necessary to review the resistance standard against the pulling force in the vertical upward direction.

Furthermore, in the case of the long period wave and breaking abrupt wave, the value β exceeded 1 and safety was confirmed. However, in the case of the short period waves and non-breaking abrupt wave, the value β turned out to be negative, far smaller than 1 because the vertical wave forces exceeded the weight of the superstructure. Thus, it was considered to be risky.

Tab. 4 Ratio of tsunami wave forces acting on a real bridge and value β

Wave force direction	Horizontal	Vertical upward	value β
Short period wave 1	0.51	1.44	-0.51
Short period wave 2	0.45	1.19	-0.25
Short period wave 3	0.50	1.11	-0.13
Long period wave	0.31	0.43	1.11
Breaking abrupt wave	0.85	1.13	-0.09
Non-breaking abrupt wave	0.25	0.27	1.75

Observations

In this study, findings about tsunami wave forces acting on the standard two-lane PC box girder sectional surface in Japanese expressway are as follows:

(1) The forces acting on the bridge superstructure are different greatly depending on the type of tsunami. For the wave force characteristics of tsunami, the wave forces in the vertical direction are larger than the wave forces in the horizontal direction except breaking abrupt wave.
(2) The magnitude of horizontal wave forces may be evaluated indirectly by gradient of wave front.
(3) Based on the calculations of tsunami wave forces acting on a actual scale bridge and their comparison with the seismic design standard of the shoe in Japanese, it turned out to be necessary to review safety procedures against lift due to pulling out caused by vertical upward wave forces. Especially, it was judged that the short-period waves and non-breaking abrupt waves would cause washout of the superstructure because the ratio of the vertical wave forces to the weight of the superstructure became 1 or larger and the value β (the ratio of resistance force of the girder to the maximum horizontal wave forces) became less than 1.

In this study, the box girder bridge was discussed. However, because the tsunami wave force characteristics are supposed to vary depending on the cross-sectional form, etc., the author plans to study the wave forces acting on the girder of other forms such as a plate girder bridge.

References

1) *Tsunami damage evaluation of Kesen Bridge by iamge and numerical analysis method* by Jinguji, Kousa, Sasaki and Sato; Journal of Structural Engineering Vol. 60A (March, 2014)
2) *Estimated washout mechanism of Utatsu Oohashi Bridge by image analysis* by Ami Nakano, Kenji Kousa, Tatsuo Sasaki and Li Fu; Proceedings of The 15th Symposium on seismic design of bridges and others based on performances; pp. 17-24, 2012.
3) Damage analysis of bridge based on the ratio of resistance force of the girder and acting force of the tsunami by Sasaki, Kousa and Yu Zheng; Journal of Structural Engineering Vol. 59A (March, 2013)
4) *Friction coefficient of steel on concrete or grout*, by Rabbat, B.G. and Russel, H.G.; Journal of Structural Engineering, ASCE, Vol. 111, No. 3, pp. 505-515, 1985.